Na$_2$IrO$_3$ as a molecular orbital crystal

I. I. Mazin,[1] Harald O. Jeschke,[2] Kateryna Foyevtsova,[2] Roser Valentí,[2] and D. I. Khomskii[3]

[1]*Code 6393, Naval Research Laboratory, Washington, DC 20375, USA*
[2]*Institut für Theoretische Physik, Goethe-Universität Frankfurt, 60438 Frankfurt am Main, Germany*
[3]*II. Physikalisches Institut, Universität zu Köln, Zülpicher Straße 77, 50937 Köln, Germany*
(Dated: September 18, 2012)

Contrary to previous studies that classify Na$_2$IrO$_3$ as a realization of the Heisenberg-Kitaev model with dominant spin-orbit coupling, we show that this system represents a highly unusual case in which the electronic structure is dominated by the formation of quasi-molecular orbitals (QMOs), with substantial quenching of the orbital moments. The QMOs consist of six atomic orbitals on an Ir hexagon, but each Ir atom belongs to three different QMOs. The concept of such QMOs in solids invokes very different physics compared to the models considered previously. Employing density functional theory calculations and model considerations we find that both the insulating behavior and the experimentally observed zigzag antiferromagnetism in Na$_2$IrO$_3$ naturally follow from the QMO model.

High interest in the recently synthesized hexagonal iridates [1–3] is due to the hypothesis [4, 5] that the electronic structure in these materials is dominated by the spin-orbit (SO) interaction. In this case, the Ir t_{2g} bands are most naturally described by relativistic atomic orbitals with the effective angular moment, $j_{\rm eff} = 3/2$ and $j_{\rm eff} = 1/2$. In this approximation, the splitting between the 3/2 and 1/2 states is larger than their dispersion. The upper band $j_{\rm eff} = 1/2$ is half filled and Ir atoms can be described as localized ($j_{\rm eff} = 1/2$, $M = 1$ $\mu_{\rm B}$) magnetic moments [6] with the exchange interaction strongly affected by SO coupling. In particular, this picture leads to a very appealing framework known as Heisenberg-Kitaev model [7, 8], with highly nontrivial physical properties. However, experimental evidence for the $j_{\rm eff}$ scenario is lacking [9].

In this Letter, based on *ab initio* density functional theory (DFT) calculations and model considerations, we show that this picture does not apply to the actual Na$_2$IrO$_3$. Instead, this system represents a highly unusual case where the formation of electronic structure is dominated by quasi-molecular orbitals (QMOs), which involve six Ir atoms arranged in a hexagon. What distinguishes this picture from molecular solids is that there is no associated spatial clusterization, but each Ir atom (via its three t_{2g} orbitals) participates in three different QMOs, yet in the first approximation there is no inter-QMO hopping the thus formed bands are dispersionless.

Such an electronic structure calls for a new approach. There is no known recipe for handling its magnetic properties, or adding Coulomb correlations, for instance. While we will not present a complete theory of spin dynamics and correlations in the QMO framework, we will outline the general directions and most important questions, in the expectation that this will stimulate more theoretical and experimental work and eventually generate more insight. Yet, the key observable features of

Na$_2$IrO$_3$: small magnetic moment, unusual zigzag antiferromagnetism, and Mott-enhanced insulating behavior, are naturally consistent with the QMO framework.

The main crystallographic element of Na$_2$IrO$_3$ (see SI) is an Ir^{4+} ($5d^5$) honeycomb layer with a Na^{1+} ion located at its center. Each Ir is surrounded by an O octahedron, squeezed along the cubic [111] (hexagonal z) axis. Therefore, Ir d-states are split into an upper e_g doublet and a lower t_{2g} triplet. The [111] squeezing further splits the t_{2g} levels into a doublet and singlet; initially this effect was neglected [4, 7, 8], however, it was later included [10, 11] (and overestimated) to explain the observed deviations from the Heisenberg-Kitaev model.

In the previous works, after identifying the $t_{2g} - e_g$ splitting it was assumed that the energy scales are $W < (J_H, \lambda) < U$, where $W \sim 4t$ is the d-electron band width, t the effective hopping parameter, J_H the Hund's rule coupling, λ the SO parameter, and U the on-site Coulomb repulsion. In this limit, the electrons are localized and the system is a Mott insulator. While $\lambda \sim$ 0.4-0.5 eV for $5d$ ions, the bandwidth for $5d$ orbitals is 1.5-2 eV and $U \sim 1 - 2$ eV, $J_H \sim 0.5$ eV, reduced compared to typical $U \sim 3 - 5$ eV and $J_H \sim 0.8 - 0.9$ eV for $3d$ electrons. Many-body renormalization may narrow the bands by a factor (m^*/m); however, given that in Ir $U \sim W$, it is unrealistic to expect a large renormalization. Therefore, the usual starting point $W < (J_H, \lambda) < U$ is not valid here, rather, the system is close to an itinerant regime. *I.e.*, one cannot justify reducing the description of Na$_2$IrO$_3$ (and possibly other iridates) to an effective $j = 1/2$ model, decoupled from the other j_{eff} states.

Thus, the first step (usually skipped) is to understand the non-relativistic band structure. We have therefore performed DFT calculations (see SI) initially without SO effects (see Fig. 1, solid purple lines). Inverting the band structure results (see SI), we obtained the corresponding tight-binding Hamiltonian. The leading channel (by far)
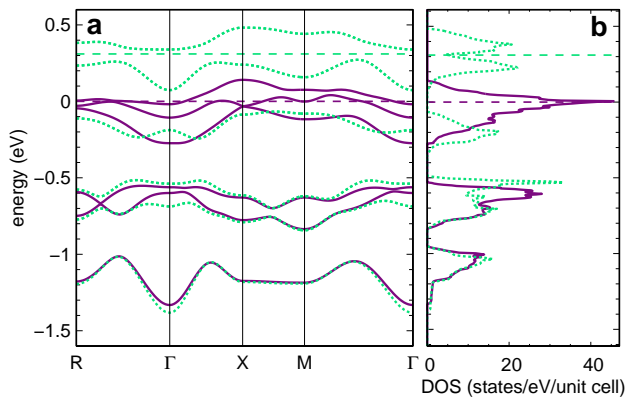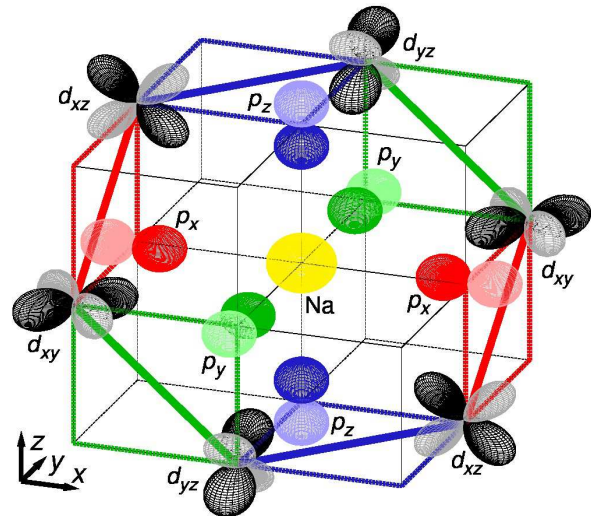
FIG. 1: (color online) Electronic structure of the non-magnetic Na_2IrO_3 for the experimentally determined [12] crystal structure. The calculations were performed with the full potential local orbital (FPLO) basis using the generalized gradient approximation (see SI). The solid purple and dotted green lines refer to calculations without and with SO interaction, respectively. Note that the Fermi levels (shown by the horizontal dotted lines) are not aligned.

FIG. 2: (color online) Most relevant O p-assisted hopping paths in idealized Na_2IrO_3 structure. For each of the three Ir-Ir bond types only hopping between two particular t_{2g} orbitals is possible. The same holds for the second and third nearest neighbor hopping via O p and Na s orbitals. Ir-Ir bonds are color coded as follows: xy bonds are shown by blue lines, xz bonds by green, and yz bonds by red ones.

is the nearest neighbor (NN) O-assisted hopping between unlike orbitals (see Fig. 2). This was also correctly identified previously [4, 5]. There are three different types of NN Ir-Ir bonds; for one (we name it xy bond) (see Fig. 3) this hopping is only allowed between d_{xz} and d_{yz} orbitals, for the next (xz) between d_{yz} and d_{xy} orbitals and for the third bond (yz) between d_{xy} and d_{xz}. In our calculations this hopping, t'_1 (the prime indicates that the hopping is via O) is about 270 meV. Perturbatively, this term is proportional to $t^2_{pd\pi}/(E_{t_{2g}} - E_p)$, where p stands for the O p states. Ref. [5] pointed out another (next nearest neighbors, NNN) O-assisted term, which we find to be ~ 75 meV. Jackeli and Khalliulin [4] invoked another NN hopping process, between like orbitals pointing directly to each other. Despite the short Ir-Ir distance, these matrix elements are surprisingly small, $\lesssim 30$ meV. Finally, some authors [10, 11] addressed the trigonal squeeze, which creates non-zero matrix elements between the same-site t_{2g} orbitals.

The main feature of the calculated non-relativistic band structure (see Fig. 1) is formation of a singly degenerate (not counting spins) band state at ~ -1.2 eV, a doubly degenerate one at -0.7 eV, and a three-band manifold between -0.3 and 0.2 eV. This clear separation, of the order of 0.3 eV, cannot be related to the trigonal squeeze, as this can only split the 6 t_{2g} bands (there are two Ir per cell) into a doublet and quartet.

In order to understand this, we start with the dominant hopping, the NN O-assisted t'_1. Let us consider an electron on a given Ir site in a particular orbital state, say, d_{xz}. The site has three NN neighbors. As discussed above, this electron can hop, with the amplitude t'_1, to a

neighboring state of d_{yz} symmetry, located at a particular NN site. From there, it can hop further into a d_{xy} state on the next site, and so on (see Figs. 2 and 3). At each site, the electron has only one bond along which it can hop. Following the electron around, we see that after six hops it returns to the same state and site from where it started. *This means that in the NN t'_1 approximation every electron is fully localized within 6 sites forming a hexagon.* Such a state could be called a molecular orbital, except that there are no spatially separated molecules on which electrons are localized. Each Ir belongs to three hexagons, and each Ir-Ir bond to two. Thus, three different t_{2g} orbitals on each Ir site belong to three different "quasi-molecular" orbitals (QMO) and these QMOs are fully localized in this approximation (Fig. 3).

Six QMOs localized on a particular hexagon form six levels, listed in Table I, grouped into the lowest B_{1u} singlet, the highest A_{1g} singlet, and two doublets E_{1g} and E_{2u}. The energy separation between the lowest and the highest level is $4t'_1$, which is close to the calculated total non-relativistic t_{2g} band width.

We now add the O-assisted NNN hopping t'_2. Here there are several such paths. However, the dominant hopping takes advantage of the diffuse Na s orbital (see Fig. 2), and is proportional to $t^2_{pd\pi}t^2_{sp}/(E_{t_{2g}} - E_p)^2(E_{t_{2g}} - E_s) < 0$. It connects unlike NNN t_{2g} orbitals that belong to the same QMO, and therefore retains the complete localization of individual QMOs. It does shift the energy
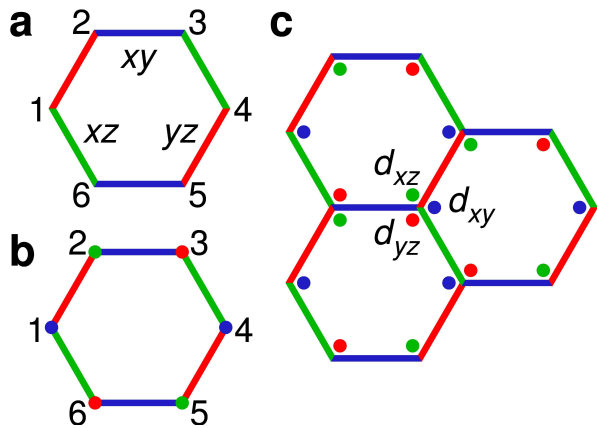
FIG. 3: (color online) (a) Schematic plot of a Ir$_6$Na hexagon. We use the same color coding as in Fig. 2, xy bonds are shown by blue lines and d_{xy} orbitals by blue dots, *etc*. (b) A quasi-molecular composite orbital on a given hexagon. (c) Three neighboring quasi-molecular orbitals.

TABLE I: Six quasi-molecular orbitals formed by the six t_{2g} atomic orbitals on a hexagon. ($\omega = \exp(i\pi/3)$). Note that $t'_1 > 0$ and $t'_2 < 0$

Symmetry	Eigenenergy	Eigenvector(s)
A_{1g}	$2(t'_1 + t'_2)$	$(1, 1, 1, 1, 1, 1)$
E_{2u}	$t'_1 - t'_2$	$(1, \omega, \omega^2, -1, \omega^4, \omega^5)$
(twofold)		$(1, \omega^5, \omega^4, -1, \omega^2, \omega)$
E_{1g}	$-t'_1 - t'_2$	$(1, \omega^2, \omega^4, 1, \omega^2, \omega^4)$
(twofold)		$(1, \omega^4, \omega^2, 1, \omega^4, \omega^2)$
B_{1u}	$-2(t'_1 + t'_2)$	$(1, -1, 1, -1, 1, -1)$

levels though, as shown in Table I. The upper singlet and doublet get closer and the lower bands move apart providing the average energy separations of ~ 0.5, ~ 0.6, and ~ 0.1 eV among the calculated non-relativistic subbands (at $|t'_1/t'_2| = 2$ the upper two levels merge; in reality, $|t'_1/t'_2| \approx 3.3$). Given that the subband widths are 0.2–0.3 eV, obviously, the upper doublet and singlet merge to form one three-band manifold.

Several effects contribute to the residual dispersion of the QMO subbands. The trigonal splitting plays a role, albeit smaller than often assumed: the trigonal hybridization is $\Delta \approx 25$ meV (the splitting being 3Δ). This may seem surprising, given the large distortion of the O octahedra, however, in triangular layers several factors of different signs contribute to Δ, and strong cancellations are not uncommon[13]. Trigonal splitting, combined with various NN and NNN hoppings not accounted for above, all of them on the order of 20 meV, trigger subband dispersions of 200–300 meV (see SI for further discussion).

We shall now address the SO interaction. The corresponding bands and density of states (DOS) are shown

in Fig. 1. The lowest two subbands hardly exhibit any SO effect, even though the spin-orbit parameter λ in Ir is $\sim$ 0.4-0.5 eV, larger than both the subband widths and subband separation. However, a simple calculation shows that not only are the orbital momentum matrix elements between the QMOs on the same hexagon zero (this follows from the quenching of the orbital momentum in the QMO states), but they also vanish between the like QMOs, located at the neighboring hexagons, such as $B_{1u} - B_{1u}$. Furthermore, at Γ the matrix elements between the two lowest subbands, B_{1u} and E_{1g}, vanish because of different parities; away from the Γ point the effect of SO increases, in the first approximation, as $F(\mathbf{k}) = \sin^2 \mathbf{kA} + \sin^2 \mathbf{kB} + \sin^2 \mathbf{kC}$, where $\mathbf{A}$, $\mathbf{B}$ and $\mathbf{C}$ are the three vectors connecting the centers of the hexagons, as can be worked out by applying the $\mathbf{L} \cdot \mathbf{S}$ operator to the corresponding QMOs.

The situation becomes more complex in the upper manifold, where three bands, A_{1g} and two E_{2u}, come very close. Even though the diagonal matrix elements, as well as nondiagonal elements at Γ still vanish, the fact that A_{1g} and E_{2u} are nearly degenerate in energy induces a considerable SO effect at all other $\mathbf{k}$-points (which grows linearly with k, as $\sqrt{F(\mathbf{k})}$). Note that deviations from the minimal model (t'_1, t'_2) and SO coupling with the lower E_{1g} states also affect the bands at $k = 0$. We also remind that the orbital moment of the individual electronic states can only be finite if the QMOs mix (which is the case), and the direction of the orbital moment is different in different parts of the Brillouin zone: along one of the three cardinal in-plane directions it is parallel to the cubic x, along another to y, *etc*. Since the spin moment tends to be parallel to the orbital moment, SO is competing with the Hund's rule coupling and suppresses the tendency to magnetism.

Let us now discuss the effect of the Hubbard correlations. It was initially conjectured that Na$_2$IrO$_3$ was a Mott insulator. This seems counterintuitive, since similar $4d$ Ru and Rh compounds are correlated metals, and more diffuse $5d$ orbitals have a smaller Hubbard $U \sim 1.5 - 2$ eV and stronger hybridization. It is hard to justify that this U can drive a 5/6 filled band of a similar width into an insulating state. Recently another, more logical concept has gained currency: on the LDA level Na$_2$IrO$_3$ is a semimetal, barely missing being a semiconductor, and a small Hubbard U just helps to enhance the already (spin-orbit driven) existing gap. Indeed, in our calculations the minimal gap is -8 meV, but the average direct gap is 150 meV, consistent with the optical absorption[14]. The minimal direct (optical) gap is 50 meV, so it is plausible that it is somewhat enhanced by correlation effects.

In order to include the effect of an onsite Hubbard U in the QMO basis, a $U_{\mathrm{QMO}} \sim U/6$ has to be applied to each QMO[15], with a residual Coulomb repulsion between neighboring QMOs, $V_{\mathrm{QMO}} \sim U/18 = U_{\mathrm{QMO}}/3$

(note that two QMOs overlap on two sites). Overall, we expect that the effect of the Coulomb repulsion in our system is similar to that in a single-site two-orbital Hubbard model at half filling (the upper QMO band is half-filled) and $U_{QMO} \approx W \approx 150 - 200$ meV. In this case, since U_{QMO} does not compete with one-electron hopping any more, one should expect that the gap will be enhanced by a considerable fraction of U_{QMO}, which is consistent with the experiment. Thus, Hubbard correlations are of no qualitative importance, and only moderately enhance the existing gap.

Since all electrons are fully delocalized over six sites, any model assuming localized spins (whether Heisenberg or Kitaev) is difficult to justify. On the other hand, the QMOs are not magnetically rigid objects and neighboring QMOs overlap on 2 out of 6 sites, which makes a model with magnetic moments localized on QMOs equally unsuitable [16].

We will consider therefore magnetism in the itinerant approach. In the non-relativistic case, the non-magnetic DOS shows a high peak at E_F due to E_{2u} and A_{1g} merging and rather flat band dispersion (see Fig. 1). Such a system is unstable against ferromagnetism (FM) and the peak is easily split gaining exchange energy (1 μ_B/Ir) with little loss of kinetic energy. The resulting FM state is half-metallic (Fig. 4) (see SI).
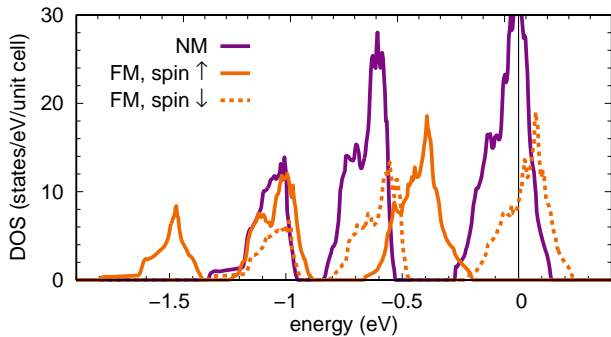

FIG. 4: Non-relativistic non-magnetic (purple) and ferromagnetic (orange) density of states (DOS) of Na_2IrO_3 calculated with the FPLO basis.

Turning on the SO interaction has a drastic effect on magnetism. SO competes with the Hund's rule that favors all onsite orbitals to be collinear. The spin moment is then reduced from 1 μ_B to ≈ 0.4 μ_B/Ir for ferro-, and ≈ 0.2 μ_B/Ir for the zigzag and stripe antiferromagnetic (AFM) arrangements (see SI). The orbital moment is parallel to the spin one, reminiscent of the $j_{eff} = 1/2$ state, and is roughly equal in magnitude and not twice larger, as it should be for $j_{eff} = 1/2$. The energy gain for the FM case drops to a few meV/Ir [17], and the zigzag pattern evolves as the most favorable AFM state.

Qualitatively, two closely competing ground states emerge from the relativistic DFT calculations: ferromagnetic and zigzag. In the context of an itinerant picture,

we can argue as follows. SO creates a pseudogap at the Fermi level in the non-magnetic calculations (see Fig. 1). This gains one-electron energy and any AFM arrangement that destroys this pseudogap incurs a penalty. From the three considered AFM states only zigzag preserves (even slightly enhances) the pseudogap (see SI). That gives this state an immediate energetical advantage and leads to the energy balance described above. Two notes are in place: first, all the above holds in LDA+U calculations with a reasonable atomic U (we have checked U up to 3.8 eV). The role of U in these systems - as stated previously- is merely enhancing the existing SO-driven gap. Second, if the DOS indeed plays a decisive role in magnetic interactions, it is unlikely that they can be meaningfully mapped onto a short-range exchange model, Heisenberg or otherwise.

Summarizing, our DFT calculations demonstrate that Na_2IrO_3 is close to an itinerant regime. The electronic structure of this system is naturally described on the basis of quasi-molecular orbitals centered each on its own hexagon. This makes this, and similar materials rather unique. Proceeding from this description one can understand the main properties of Na_2IrO_3, including its unique zigzag magnetic ordering with small magnetic moment.

However, the main goal of our work is not a complete understanding of the magnetic properties of Na_2IrO_3. We realize that this understanding is still incomplete and that full explanation of the weak antiferromagnetism, as well as of the magnetic response in this compound remains a challenge. Rather, we lay out the framework in which this challenge has to be resolved. We demonstrate that both the simplified (but correct) TB model proposed in previous studies [4, 5], and full *ab initio* calculations provide a framework that is best described by the quasi-molecular orbitals. This is an as yet unexplored concept (as opposed to molecular orbitals or atomic orbitals), and there are many open questions about how to treat correlations, magnetic response *etc.* in this framework, however, it appears to be the only way to reduce the full 12 atomic orbitals (t_{2g} or their relativitsic combinations) problem to a smaller subspace ($3 \times 2 = 6$) QMOs.

[1] I. Felner and I.M. Bradaric, Physica B **311**, 195 (2002).

[2] H. Kobayashi, M. Tabuchi, M. Shikano, H. Kageyama and R. Kanno, J. Mater. Chem. **13**, 957 (2003).

[3] Y. Singh and P. Gegenwart, Phys. Rev. B **82**, 064412 (2010).

[4] G. Jackeli, and G. Khaliullin, Phys. Rev. Lett. **102**, 017205 (2009).

[5] A. Shitade, H. Katsura, J. Kuneš, X.-L. Qi, S.-C. Zhang, and N. Nagaosa, Phys. Rev. Lett. **102**, 256403 (2009).

[6] Note that in this case the spin magnetic moment is $1/3$ μ_B and the orbital moment is $2/3$ μ_B.

[7] J. Chaloupka, G. Jackeli, and G. Khaliullin, Phys. Rev. Lett. **105**, 027204 (2010).

[8] J. Reuther, R. Thomale, and S. Trebst, Phys. Rev. B **84**, 100406(R) (2011).

[9] While in recent XAS measurements (J.P. Clancy *et al.* arXiv:1205.6540) a non-zero branching ratio was reported in Na_2IrO_3, this observation only indicates that there is a substantial correlation between the spin and the orbital moments direction, $< \mathbf{L} \cdot \mathbf{S} > \neq 0$, but this fact *per se* does not tell us that relativistic atomic orbitals $j_{\text{eff}} = 1/2, 3/2$ form a good basis for describing the electronic structure. As we show in the Letter, because of an accidental degeneracy of the three top *molecular* orbitals, the effect of SO is substantial, but are not necessarily described in terms of a particular j_{eff}.

[10] C. H. Kim, H.S. Kim, H. Jeong, H. Jin, and J. Yu, Phys. Rev. Lett. **108**, 106401 (2012).

[11] S. Bhattacharjee, S.-S. Lee and Y. B. Kim, New J. Phys. **14,** 073015 (2012).

[12] S. K. Choi, R. Coldea, A. N. Kolmogorov, T. Lancaster, I. I. Mazin, S. J. Blundell, P. G. Radaelli, Y. Singh, P. Gegenwart, K. R. Choi, S.-W. Cheong, P. J. Baker, C. Stock, and J. Taylor, Phys. Rev. Lett. **108**, 127204 (2012).

[13] D. Pillay, M. D. Johannes, I. I. Mazin, O. K. Andersen, Phys. Rev. B **78**, 012501 (2008).

[14] R. Comin, G. Levy, B. Ludbrook, Z.-H. Zhu, C.N. Veenstra, J.A. Rosen, Yogesh Singh, P. Gegenwart, D. Stricker, J.N. Hancock, D. van der Marel, I.S. Elfimov, A. Damascelli, arXiv:1204.4471 (unpublished).

[15] Compare to Mott-Hubbard transition in fullerides: O. Gunnarsson. *Alkali-doped fullerides: narrow-band solids with unusual properties*. World Scientific, 2004.

[16] Spin dynamics can be in principle always mapped onto a localized spin model of a sufficient range, but this can be a dangerous exercise: compare the Fe pnictides, where such mapping led to an unphysically drastic temperature dependence of the Heisenberg exchange parameters, until it was realized that proper mapping requires a strong biquadratic term (A.L. Wysocki, K. D. Belashchenko, and V.P. Antropov, Nature Physics **7**, 485 (2011)).

[17] Incidentally, the ferromagnetic state in relativistic calculations acquires substantial anisotropy. Depending on the polarization direction, the energy gain over the nonmagnetic state varies by a factor of two. This is consistent with the experimentally observed substantial anisotropy of the uniform susceptibility in the paramagnetic state [3].

SUPPLEMENTARY INFORMATION

We performed density functional theory (DFT) calculations considering various full potential all electron codes, such as WIEN2k [S1], ELK [S2], and FPLO [S3] using the generalized gradient approximation functional in its PBE form [S4], and verified that the results agree reasonably well among different codes. Such comparison is particularly important because the codes implement the spin-orbit coupling in slightly different ways, employing usually unimportant, but in principle unequal approximations. In the *non-relativistic* calculations the core electrons were treated fully relativistically and the valence electrons non-relativistically (scalar relativistic approximation). In the *fully relativistic* calculations, *i.e.* with inclusion of spin-orbit coupling, all electrons were treated fully relativistically. We considered the $C2/m$ crystal structure as given in Ref. S5 and shown in Fig. S1.

FIG. S1: Crystal structure of Na_2IrO_3 in the cubic setting. The hexagonal direction is along the [111] direction in this setting. Ir, O and Na atoms are shown as grey, magenta, and yellow spheres, respectively. The three inequivalent Ir-Ir bonds are labeled according to their cubic directions.
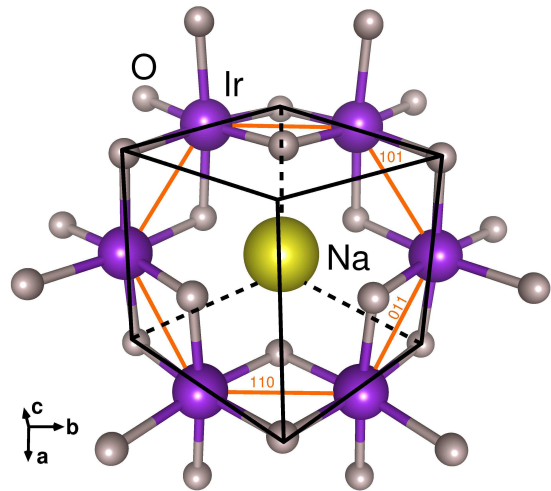
We used projective Wannier functions as implemented in the FPLO basis [S6] to determine a tight-binding (TB) representation for the Ir $5d$ bands. In Figure S2 we show the DFT band structure together with the bands corresponding to the Wannier representation and the TB bands derived from this representation.

In Fig. S3 we present the projective Wannier functions for the $5d$ orbitals of one Ir site. The Wannier functions exhibit the typical shape of the $5d$ functions at the Ir site. Besides, they show a clear asymmetry due to Na as well as tails on the O sites.

In order to analyze the contribution to the non-relativistic band structure of the various tight-binding
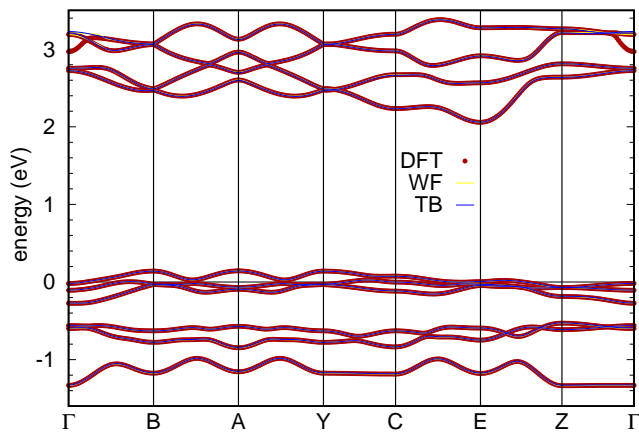
FIG. S2: Non-relativistic non-magnetic band structure of Na$_2$IrO$_3$ (red symbols) shown together with the Wannier bands (yellow) and the tight-binding bands (blue).

hopping parameters and its relation to the quasi-molecular orbital (QMO) picture, we present in Fig. S4 the band structure that results if we restrict the tight-binding Hamiltonian to first neighbors (top left), up to second nearest neighbors (top right), up to third nearest neighbors (bottom left), and without restriction (bottom right). One can see that already the second neighbors model provides a good semiquantitative description of the band formation.

In the next Figure S5 we show the tight-binding band structures within the QMO model. In these calculations we have included the on-site trigonal splitting (the top left panel), adding the nearest neighbors t'_1 hopping (top right), then the second nearest neighbors t'_2 hopping (bottom left) and, finally, including also the third nearest neighbors hopping between the like orbital, which also proceeds through Na and does not take an electron out of the corresponding QMO (bottom right). The small dispersion that arises for nearest neighbors is due to deviations from the perfect octahedral environment of iridium. Upon inclusion of second nearest neighbors, as mentioned in the main text, the upper doublet and singlet merge to form one three-band manifold.

In Figure S6, we show projections of the total density of states of Na$_2$IrO$_3$ onto the quasi-molecular orbitals specified in Table [1] of the main text. The eigenvector matrix

$$U = \begin{pmatrix} 1 & 1 & 1 & 1 & 1 & 1 \\ 1 & \omega & \omega^2 & -1 & \omega^4 & \omega^5 \\ 1 & \omega^5 & \omega^4 & -1 & \omega^2 & \omega \\ 1 & \omega^2 & \omega^4 & 1 & \omega^2 & \omega^4 \\ 1 & \omega^4 & \omega^2 & 1 & \omega^4 & \omega^2 \\ 1 & -1 & 1 & -1 & 1 & -1 \end{pmatrix}$$

(with $\omega = \exp(i\pi/3)$) is a unitary transformation that rotates the atomic Ir t_{2g} orbitals into the QMO orbital

space. E_{1g} and E_{2u} states are perfectly degenerate in the nonrelativistic case (Figure S6 (a)). When spin-orbit coupling is turned on (Figure S6 (b)), interestingly, the three upper bands are no more equivalent in this sense, with the central band being mostly A_{1g}, and the other two mostly E_{2u}. Importantly, there is hardly any mixing between the lower three bands and the upper three bands, emphasizing the fact that the low-energy physics is nearly exclusively defined by the upper three QMOs, and their mutual interaction, whether with or without spin-orbit. At the same time, one can, alternatively, project the same bands onto the relativistic orbitals, $j_{eff} = 1/2$ and $j_{eff} = 3/2$, and, as observed before[S7], the upper two bands have more $j_{eff} = 1/2$ character than $j_{eff} = 3/2$ character, but, for instance, at the $Gamma$ point, only slightly so (more at some other points). Thus, even though the SO effects are considerable, they are not strong enough to reduce the problem to a two $j_{eff} = 1/2$ model.

The magnetic patterns considered in our non-relativistic and fully relativistic calculations are shown in Fig. S7.

The ferromagnetic state shows in the absence of SO an energy gain of nearly 80 meV per Ir with respect to the non-magnetic solution and about half this value against competing antiferromagnetic states (zigzag and stripy phases); the simple Néel state is much higher in energy. Inclusion of SO changes the energetics considerably, as described in the main text, with the zigzag antiferromagnetic ordering becoming competitive with the ferromagnetic one, and lower in energy than the stripy phase. We deliberately do not discuss the calculated energies in detail, because the energy differences involved are on the order of one meV per atom, which is beyond the accuracy of the density functional theory itself, and on the border of the technical accuracy of existing band structure codes.

In Fig. S8 we show the density of states for some magnetic orderings considered in our fully relativistic calculations. Note that the zigzag ordering preserves the non-magnetic pseudogap at the Fermi level, while the stripy ordering destroys it.

Finally some considerations about the Hubbard U are at place. In fact, there are two ways of defining U in this case. As usually, the actual value of U depends on which orbitals it is being applied to. For instance, it is well known that in Fe pnictides the appropriate value of U acting on the Wannier functions combining Fe d and As p states is more than twice smaller that that acting on actual atomic d orbitals since the screening effects change depending on the basis of active states considered. In molecular solids, such as fullerides, the atomic value of U often appears completely irrelevant, and the physically meaningful value of U is the (much smaller) energy of Coulomb repulsion of two electrons placed on two molecular orbitals. In the case of Na$_2$IrO$_3$ one has a choice of
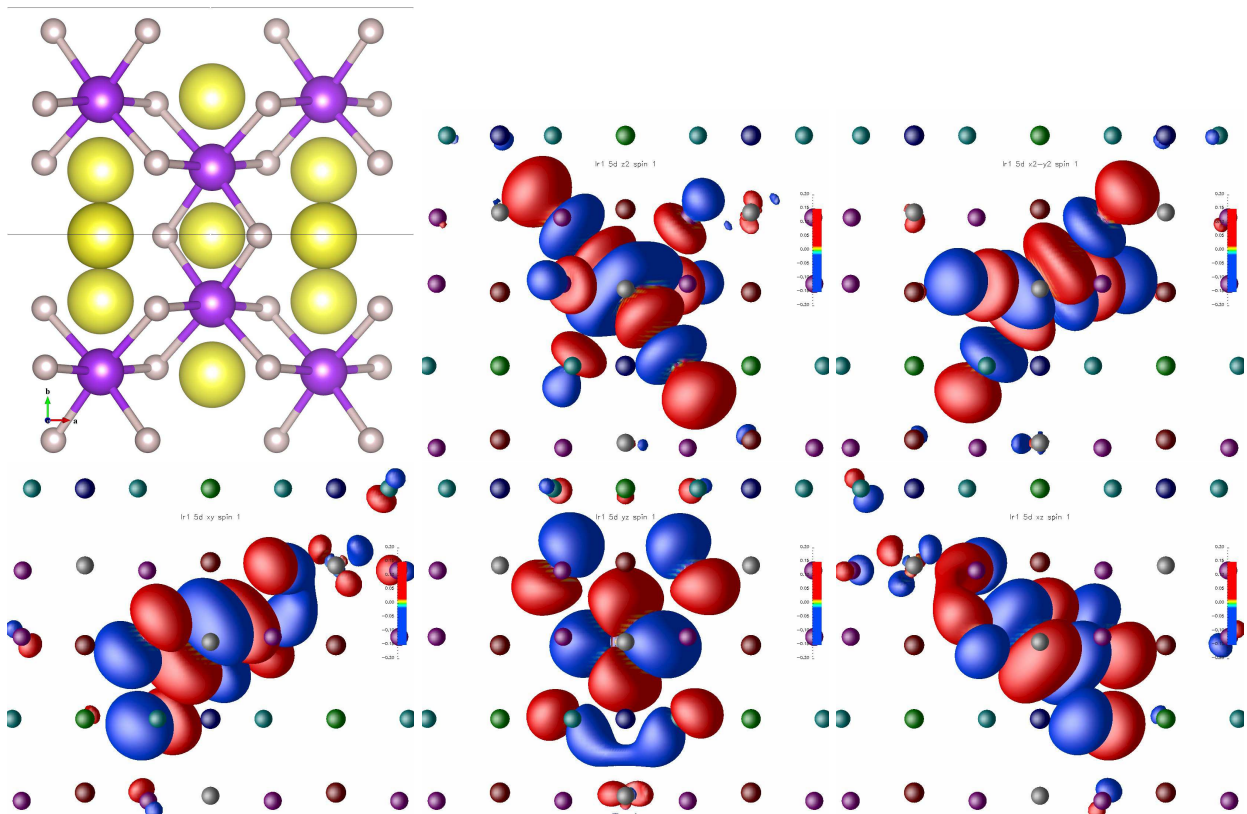
FIG. S3: Projective Wannier functions for five of the ten Ir $5d$ bands, together with a structure showing the perspective.

using an atomic $U \sim 1.5$-2 eV, realizing that the results will be strongly affected by the fact that electrons are localized not on individual ions, but on individual QMOs, or of constructing U in the QMO basis. The former way is readily available in such formalisms as LDA+U but it may be a poor choice for the description of a system based on quasi-molecular orbitals.

[S1] P. Blaha, K. Schwarz, G. K. H. Madsen, D. Kvasnicka, and J. Luitz 2001 WIEN2k, *An Augmented PlaneWave+LocalOrbitals Program for Calculating Crystal Properties* (Karlheinz Schwarz, Techn. Universität Wien, Austria).

[S2] http://elk.sourceforge.net/

[S3] K. Koepernik and H. Eschrig, Phys. Rev. B **59**. 1743 (1999); http://www.FPLO.de

[S4] J. P. Perdew, K. Burke and M. Ernzerhof, Phys. Rev. Lett. **77** 3865 (1996).

[S5] S. K. Choi, R. Coldea, A. N. Kolmogorov, T. Lancaster, I. I. Mazin, S. J. Blundell, P. G. Radaelli, Yogesh Singh, P. Gegenwart, K. R. Choi, S.-W. Cheong, P. J. Baker, C. Stock, J. Taylor, Phys. Rev. Lett. **108**, 127204 (2012).

[S6] H. Eschrig and K. Koepernik, Phys. Rev. B **80**, 104503 (2009).

[S7] A. Shitade, H. Katsura, J. Kuneš, X.-L. Qi, S.-C. Zhang, and N. Nagaosa, Phys. Rev. Lett. **102**, 256403 (2009).
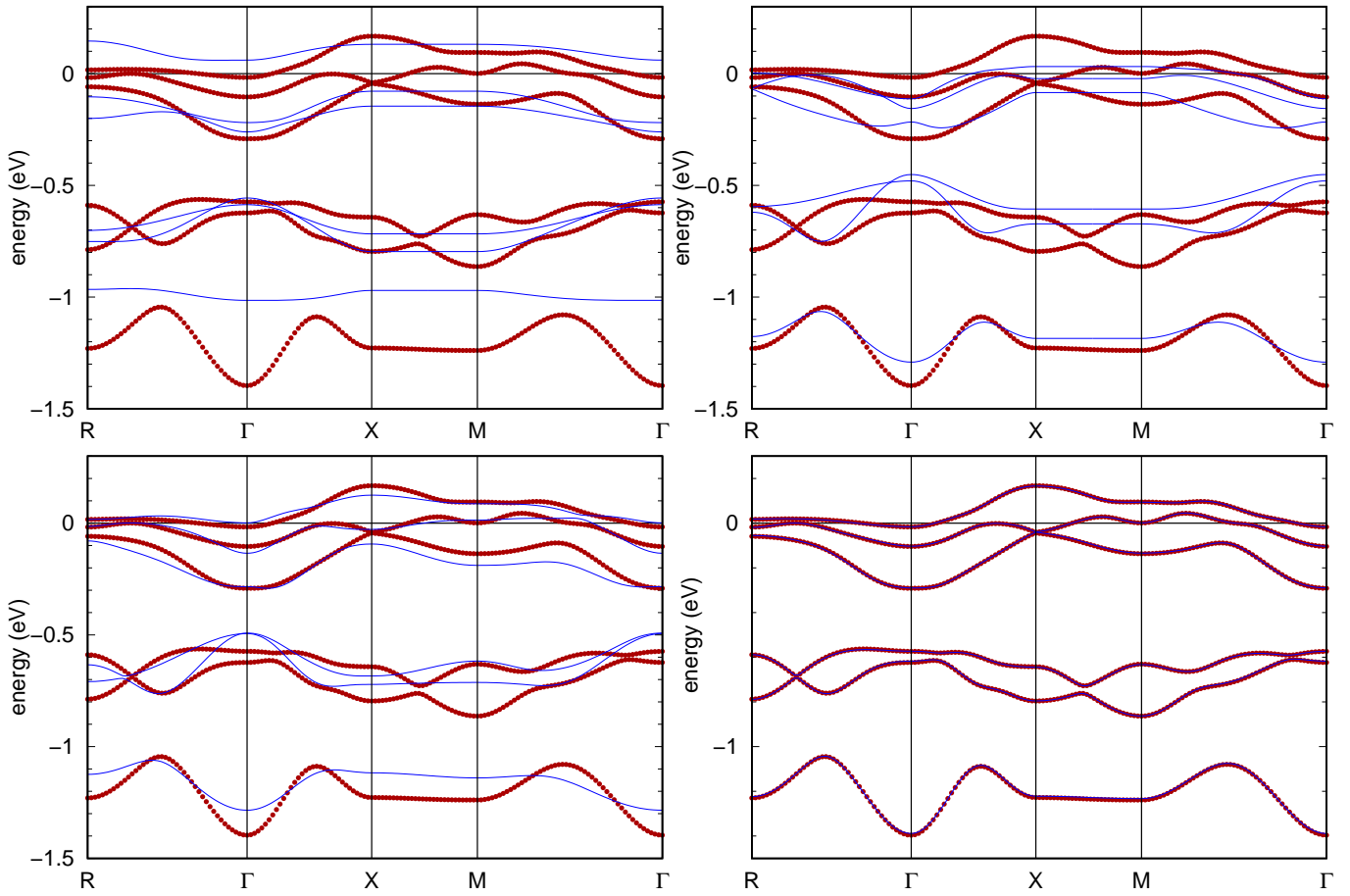
FIG. S4: Band structure of Na_2IrO_3 (red symbols) shown together with the tight-binding models that include only nearest neighbors (top left), up to next nearest neighbors (top right), up to third nearest neighbors (bottom left) and neighbors up to 16 Å (bottom right).
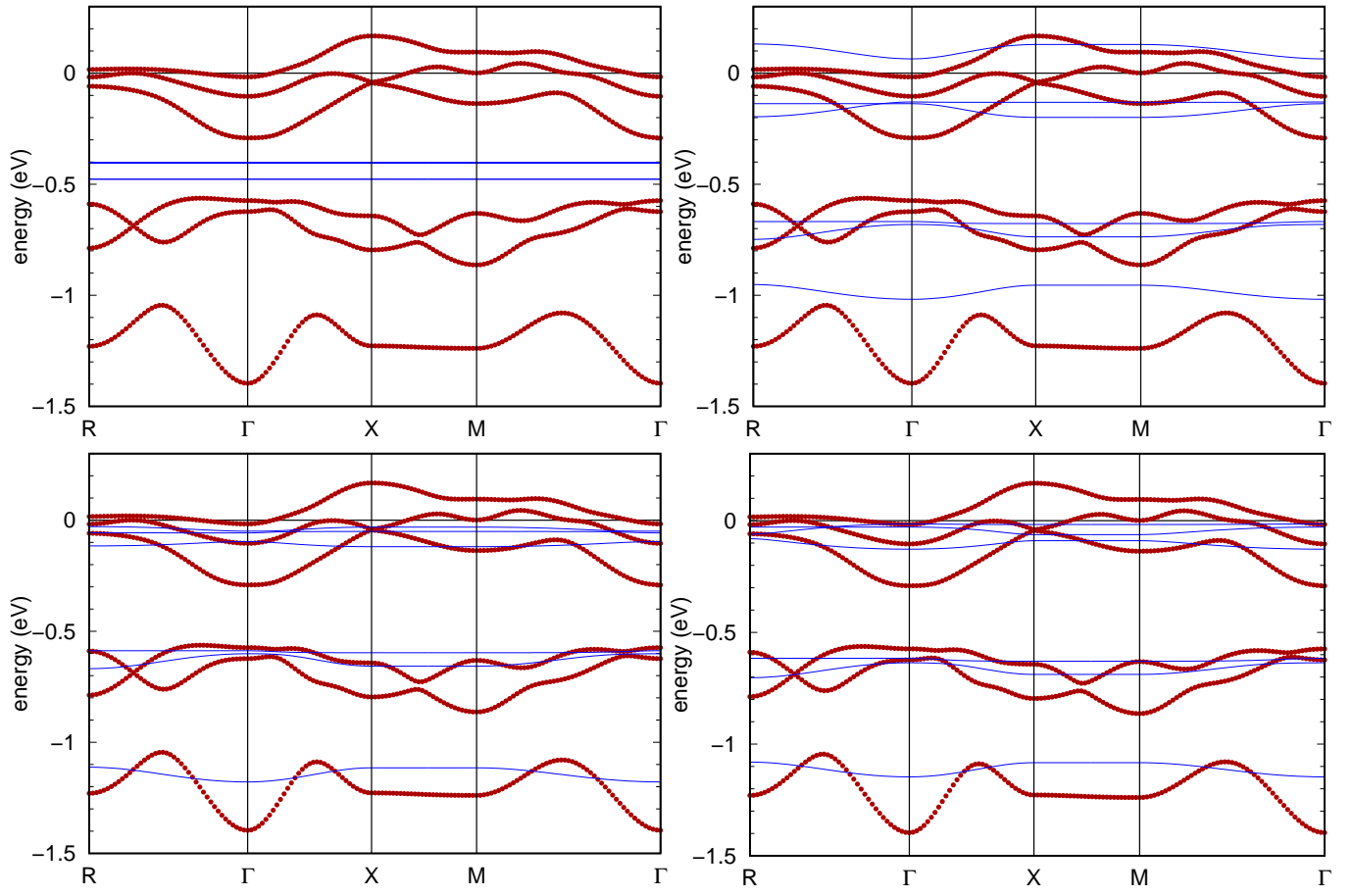
FIG. S5: Band structure of Na_2IrO_3 (red symbols) shown together with the tight-binding models that involve only parameters compatible with the quasi-molecular orbitals. Only on-site parameters (top left), up to nearest neighbors (top right), up to second nearest neighbors (bottom left) and up to third nearest neighbors (bottom right).
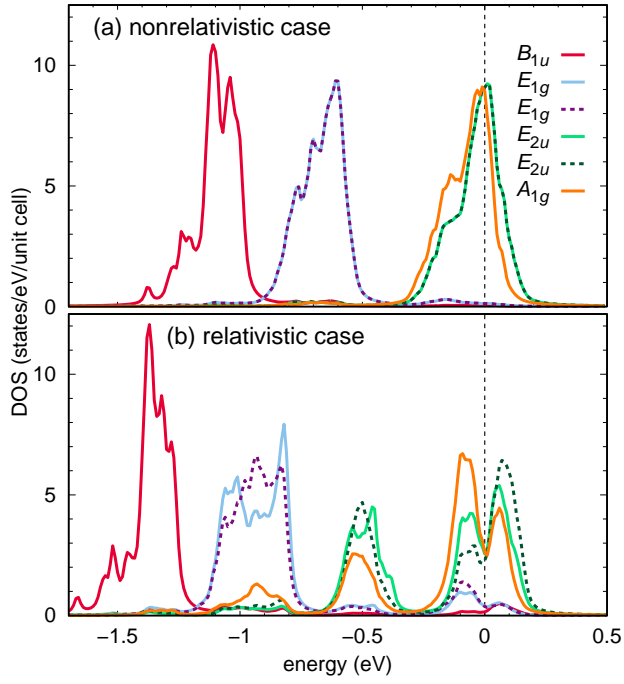
FIG. S6: Density of states of Na$_2$IrO$_3$ projected onto the six quasi-molecular orbitals given in Table [1] of the main text for (a) a nonrelativistic and (b) a relativistic calculation.
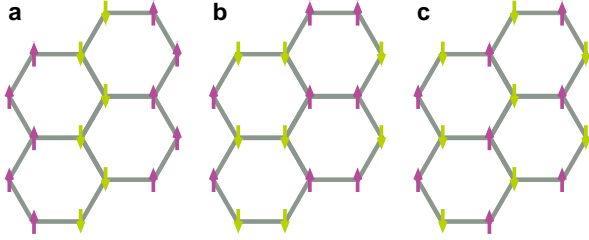

FIG. S7: Three antiferromagnetic patterns considered in this paper: (a) zigzag, (b) stripy, and (c) Néel.
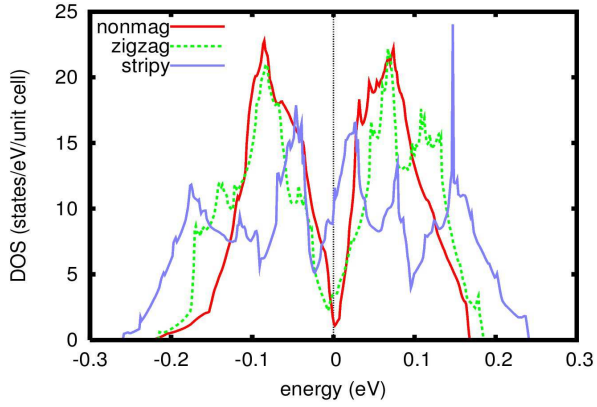

FIG. S8: Density of states, spin-orbit included, for two competing magnetic patterns compared with that for the nonmagnetic state.